LIBRARY
ROYAL AIRCRAFT ESTABLISHMENT
BEDFORD.

R. & M. No. 3376

MINISTRY OF AVIATION

AERONAUTICAL RESEARCH COUNCIL
REPORTS AND MEMORANDA

Measurements of the Direct Oscillatory Derivatives for a Linear Bending Mode on Four Rigid Half-Span Models at Subsonic and Transonic Speeds, in Closed and Slotted Tunnels

K. C. WIGHT, A.F.R.Ae.S. and MISS J. A. NIXON

LONDON: HER MAJESTY'S STATIONERY OFFICE
1964
PRICE 8*s*. 6*d*. NET

Measurements of the Direct Oscillatory Derivatives for a Linear Bending Mode on Four Rigid Half-Span Models at Subsonic and Transonic Speeds, in Closed and Slotted Tunnels

K. C. WIGHT, A.F.R.Ae.S. and MISS J. A. NIXON

*Reports and Memoranda No. 3376**

March, 1963

Summary.

Measurements have been made of the direct damping and stiffness derivatives for four rigid half-span models oscillating in a linear bending mode about an axis near the root in high-speed wind tunnels. A Mach number range of 0·6 to 1·1 was covered and the frequency parameter varied between 0·12 to 0·04. The effect of converting the slotted tunnel to a closed tunnel gave large changes in the stiffness derivatives, whilst the damping derivatives showed only small to moderate changes. Comparison with theory for the damping derivatives showed reasonable agreement, especially under closed-tunnel conditions.

LIST OF CONTENTS

* Replaces N.P.L. Aero. Report No. 1061—A.R.C. 24 650. Published with the permission of the Director, National Physical Laboratory.

LIST OF CONTENTS—*continued*

Section

---

1. *Introduction.*

The measurements described in this paper form part of a series of tests being made in the N.P.L. high-speed wind tunnels on four rigid half-models, with the object of obtaining comparisons with theory and determining conditions for which slotted-wall interference effects on oscillatory measurements are likely to be significant. It is hoped that an analysis of the results will give guidance in the design of a more systematic series of experiments aimed ultimately at the determination of actual interference corrections.

The models selected for the tests had originally been constructed for pitching measurements in the 25 in. × 20 in. High-Speed Tunnel, and are as follows:

(1) M-wing, aspect ratio 5·02

(2) Symmetrically tapered double wedge, aspect ratio 4·33

(3) Rectangular wing, aspect ratio 4·0

(4) Rectangular wing, aspect ratio 2·0.

The M-wing had been previously tested in the 25 in. × 20 in. Tunnel and measurements made of the pitching and rolling derivatives. The results indicated that the interference effects from slotted walls were considerable for the pitching damping (Ref. 1).

Measurements of the direct damping and stiffness derivatives for a rolling oscillation are discussed in this paper, both with slotted walls and with the slots sealed with adhesive tape to give closed-tunnel conditions. The tests were made by a free-oscillation method in which the motion of the model, following a disturbance, was recorded on magnetic tape. The frequency of oscillation was measured simultaneously by an electronic counter-timer. The logarithmic decrement of the motion was subsequently determined by playing back the tape record into an analyser designed to rectify and integrate selected batches of cycles (Ref. 2). With one exception, all the tests were made at a

frequency of approximately 20 c/sec; the Mach number was varied from 0·6 to 1·1 with slotted walls and to 0·85 with the slots sealed. This gave ranges of frequency parameter from 0·12 to 0·04 and of Reynolds number from $1{\cdot}5 \times 10^6$ to 4×10^6 approx.

The rectangular wing of aspect ratio 4 was the lightest of the four models and it was found possible to raise the frequency of oscillation to 33 c/sec. Tests were made at this frequency in addition to 23 c/sec for the closed-tunnel condition. All tests were made at a mean incidence of 0 degrees and the values of the derivatives correspond to mean values over the amplitude range 2° to 1°.

The measurements of damping for the closed-tunnel condition were corrected by the theory of Ref. 3 to free-stream conditions to provide a comparison with theory and with slotted-wall results (the out-of-phase loading was treated as quasi-static). Theoretical values of the derivatives were obtained by the method of Ref. 4.

2. *Description of Apparatus.*

2.1. *Details of Tunnels.*

The M-wing was tested in both the N.P.L. induced-flow wind tunnels detailed below, the remaining tests being made in the 36 in. × 14 in. Tunnel. The transonic working sections consisted of solid side walls and liners with longitudinal slots above and below the model as shown in Figs. 1 and 2. Each liner had 10 equally spaced slots and two slots of half-standard width at the side edges; one eleventh of the tunnel width was open to the plenum chamber in each case. The slots tapered from zero width at the upstream end and reached their full width in approximately 3 ft. The depth of the plenum chambers was $8\frac{1}{2}$ in. (approx.) for the 36 in. × 14 in. and $7\frac{1}{2}$ in. (approx.) for the 25 in. × 20 in. and both are open to the tunnel at the downstream end. The centre-line of the model hinge was 3 ft 9 in. from the downstream end of the slotted liners in each tunnel.

Tunnel Dimensions

Nominal Size (in.)	Actual Size of Working Section (in.)	Overall Length of Slotted Liner (ft)	Width of Slot (in.)	Width of Slat (in.)	Depth of Plenum Chamber (in.)
36 × 14	$30\frac{3}{4}$ × 14	9	0·116	1·16	$8\frac{1}{2}$
25 × 20	21 × 20	8	0·165	1·65	$7\frac{1}{2}$

Tunnel speed was obtained from measurements of static pressure at a hole in the slotted wall sufficiently far upstream to be unaffected by the presence of the model. The tunnel was calibrated without the model, using a pitot-static tube, and a number of measurements were made over the region occupied by the model both with normal slotted liners and with the slots sealed.

2.2. *Oscillation Mechanism.*

A flexure bearing shown in Fig. 3 supported the model under test and allowed a rolling oscillation about an axis outside the model area and 0·11 in. away from the root chord. The bearing was formed by four horizontal flat springs each clamped to 'earth' at one end and to a horizontal arm

at the other. These provided most of the elastic stiffness required. A pair of vertical springs supported the arm and located the axis of oscillation. A tongue extended from the root of the model and was bolted to the arm.

The model was displaced by a preset amount (2 deg) by a cranked catch moved vertically by an electric actuator and engaging with a shoulder on the horizontal arm. On reaching a stop the catch was disengaged rapidly with the aid of a toggle spring (not shown in Fig. 3) to ensure a rapid release of the model. Reversal of the actuator reset the catch for a subsequent displacement.

The flexure bearing assembly was supported on a suitable earthed mounting enclosed in an air-tight box to prevent flow into the working section of the tunnel, through the hole accommodating the model tongue.

2.3. *Measuring and Analysing Equipment.*

A variable air condenser, in which the moving vanes were displaced with the model, formed a pick-up which was used with Southern Instruments F.M. equipment to give a voltage proportional to angular displacement. This voltage was F.M. recorded on magnetic tape. The use of direct recording was unsatisfactory here because of errors introduced by 'drop-outs' and variations in tape sensitivity from point to point.

The recorded decaying oscillation was replayed into an analyser (*see* Fig. 4, reproduced from Ref. 2) in which the signal was first amplified and rectified. An electronic counter in conjunction with a relay gate then selected a batch of cycles for integration by an analogue integrator (Ref. 2).

Integrations of two or more different batches of cycles in the record, obtained on successive replay, normally give sufficient information for the determination of the logarithmic decrement of the motion.

For the measurement of period the signal from the displacement pick-up was amplified and shaped to operate an electronic counter which produced start and stop pulses for an electronic timer at the beginning and end of 10 cycles.

2.4. *Details of Models.*

Details of the four models are listed below and the planforms are illustrated in Fig. 5.

	M-Wing	Rectangular Wings		Tapered Wedge
Section	RAE 101	RAE 102	RAE 102	Double Wedge ($\lambda = 0{\cdot}266$)
Aspect ratio	5·02	2	4	4·33
Thickness/chord	6%	10%	10%	5%
Root chord (in.)	8·14	7	5	7
Mean chord (in.)	4·382	7	5	4·431
Span (in.)	11	7	10	9·59

The four models used in these tests were machined from solid steel and provided with rectangular tongues for clamping to the flexure bearing. The $A = 4$ rectangular wing was of special construction in which parts of the steel had been removed and replaced by balsa-wood inserts with resin-impregnated surfaces, the intention being to raise the flexural frequency of the model to enable high-frequency pitching measurements to be made in the future.

The models were provided with a carborundum transition band extending from the leading edge to $0 \cdot 1c$ on both surfaces, since earlier experiments in the 25 in. $\times$ 20 in. Tunnel had shown that large changes in damping could occur in the transonic region if the model boundary layer was partly laminar. In the case of the tapered double wedge a small gap was left between the sharp leading edge and the beginning of the transition band.

Each model was fitted with a root fence to cover the hole in the tunnel wall through which the model was supported and to reduce flow through the small gap between the wall and the model root.

3. *Method of Test and Analysis.*

3.1. *Measurements.*

Measurements of the damping derivatives were obtained from the determination of the logarithmic decrements under wind-on conditions and also in still air. The logarithmic decrements were obtained from individual integration of all half-cycles in the tape record, since integration of batches of cycles (Section 2.3) obscured non-linearities which were present at the higher Mach numbers.

The stiffness derivatives were obtained from the change in period of oscillation due to wind loading. The period was measured by the counter-timer for ten cycles. The small changes of period involved could not be determined with sufficient accuracy from measurements on the signal from the tape recorder on account of 'wow' and 'flutter' present in the latter.

The elastic stiffness σ was determined statically by applying known loads and measuring displacements, and dynamically by applying known inertias and measuring period changes. The values obtained were in agreement.

3.2. *Analysis.*

The aerodynamic moment about the axis of oscillation is of the form

$$B = B_{\phi}\phi + B_{\dot{\phi}}\dot{\phi} \tag{1}$$

where the coefficients are the derivatives and ϕ is the angular displacement.

The equation of motion of the model may be written

$$I\ddot{\phi} + (\kappa - B_{\dot{\phi}})\dot{\phi} + (\sigma - B_{\phi})\phi = 0 \tag{2}$$

where κ is the apparatus damping coefficient and σ is the elastic stiffness for angular displacement about the axis.

A solution of the form $\phi = \bar{\phi}e^{\mu t} \sin pt$ leads to the following expressions for the derivatives if it is assumed that $p_0^2 > > \mu_0^2$ (a condition found in practice) and that κ is hysteresis damping (*see* Section 3.3) which may be expressed in the form

$$\kappa = \frac{T}{T_0}\kappa_0 \tag{3}$$

$$B_{\phi} = \frac{\sigma}{\pi^2 T^2}[\pi^2(T^2 - T_0^2) + T^2x_0^2 - T_0^2x^2] \tag{4}$$

$$B_{\dot{\phi}} = \frac{\sigma}{\pi^2 T}[T^2x_0 - T_0^2x] \tag{5}$$

where x is the logarithmic decrement, T is the period, and suffix $_0$ denotes still-air conditions.

Non-dimensional forms of the derivatives are given by (Ref. 4)

$$b_\phi = B_\phi/\rho V^2 Ss \tag{6}$$

and

$$b_{\dot{\phi}} = B_{\dot{\phi}}/\rho V Ss^2 \tag{7}$$

and the phase angle between the aerodynamic moment and the displacement is ϵ where

$$\text{Tan } \epsilon = \frac{\bar{\nu}s}{\bar{c}} b_{\dot{\phi}}/b_\phi . \tag{8}$$

3.3. *Corrections.*

Since the pressure and density in the working section of the tunnel were not atmospheric when the tunnel was operating and depended on Mach number, tests were made to determine the still-air component of the apparatus damping by using the apparatus enclosure (*see* Section 2.2) as an air-tight chamber and covering the model with a large air-tight box. The pressure and hence density in the chamber could be varied to cover the required tunnel conditions. Results obtained indicated that the still-air component was negligible, and thus the apparatus damping could be regarded as due solely to mechanical hysteresis. This result is implied in equation (5) for $B_{\dot{\phi}}$ and no corrections to the damping are required for variations in air density.

The same tests showed small changes in still-air frequency with variation in air density, due to changes in still-air additional inertia. These results have been used to correct still-air frequencies measured under atmospheric conditions to values corresponding to the densities of the tests.

Further corrections were required for measurements involving frequency. The time interval measured by the counter-timer did not correspond to exactly 10 cycles of oscillation since the phase of the stop pulse differed from that at the start due to the decay in amplitude of the input signal; correction was made to give the time of exactly 10 cycles.

4. *Results and Discussion.*

Tests were made to determine the effectiveness of the fence by removing it in the case of the two rectangular wings and the tapered double wedge. Large changes in the measurements resulted in the case of the $A = 4$ rectangular wing and the tapered double wedge (Figs. 6 and 7), but with the $A = 2$ rectangular wing where the hole in the tunnel wall remained covered by the root profile, little change was observed (Fig. 8).

Further tests were made with the $A = 4$ rectangular wing with the fence reduced to half its original size but still covering the hole, and also with the fence removed and the hole covered with adhesive tape. These tests supported the conclusion that, in the case of flapping tests, the most important effect of the root fence was to cover the hole in the tunnel wall and thus reduce flow in and out of the working section in this region.

Experimental values of $-b_{\dot{\phi}}$ and $-b_\phi$ for closed and slotted-wall tunnels are given in Tables 1 to 5. The tables also include closed-tunnel values of $-b_{\dot{\phi}}$ corrected for tunnel interference (*see* Section 1). The latter and the slotted-wall-tunnel results are plotted against Mach number in Figs. 9 to 14. The figures also give a comparison with free-stream theoretical values for the damping derivative $-b_{\dot{\phi}}$. The theoretical value of the stiffness derivative $-b_\phi$ is zero. Attention is drawn to the main features of the results in the following sections.

4.1. *M-Wing* (*Figs.* 9 *and* 10).

The measurements of damping and stiffness derivatives in the two tunnels were in good agreement, especially for closed-tunnel conditions, and the variation with Mach number was smooth and relatively small. Comparison between slotted-wall results and those for the closed tunnel, corrected by the method of Ref. 2, showed exact agreement for the 25 in. × 20 in. Tunnel. For the 36 in. × 14 in. Tunnel with slotted walls, the damping derivative $-b_{\dot{\phi}}$ was increased by a small percentage and the stiffness derivative $-b_{\phi}$ was decreased by a somewhat greater percentage change.

The theoretical curve for $-b_{\dot{\phi}}$ is in very good agreement with the closed-tunnel results.

4.2. *Tapered Wing* (*Fig.* 11).

The slotted-wall values of $-b_{\dot{\phi}}$ showed considerable variation with Mach number, apparently rising to a peak in the neighbourhood of $M = 0{\cdot}9$. Results for the closed tunnel showed a similar trend. Below $M = 0{\cdot}8$ the slotted walls gave larger values for both $-b_{\dot{\phi}}$ and b_{ϕ} than the closed tunnel.

Theory for $-b_{\dot{\phi}}$ was in good agreement with experiment for closed-tunnel conditions at the lower end of the Mach number range, but gave lower values as the Mach number increased.

4.3. *Rectangular Wing* $A = 4$ (*Fig.* 12).

Large fluctuations in both $-b_{\dot{\phi}}$ and $-b_{\phi}$ occurred in the Mach number range $0{\cdot}8$ to $1{\cdot}0$ with a narrow region ($0{\cdot}89 < M < 0{\cdot}91$) of negative damping at $M = 0{\cdot}9$. The effect of the slotted walls below $M = 0{\cdot}8$ was similar to that for the tapered wing. Increasing the frequency of oscillation from 23 c/sec to 33 c/sec for the closed-tunnel case had negligible effect on the damping but altered the stiffness derivatives.

Theoretical values of $-b_{\dot{\phi}}$ were in good agreement with closed-tunnel results at low Mach numbers, but failed to predict the rise and rapid fall in the region of $M = 0{\cdot}8$, which could be ascribed to the formation of local supersonic regions not accounted for in the theory.

4.4. *Rectangular Wing* $A = 2$ (*Figs.* 13 *and* 14).

Similar fluctuations in $-b_{\dot{\phi}}$ and $-b_{\phi}$ to those obtained with the previous wing ($A = 4$) occur at slightly higher Mach number. In the subsonic region the increase in $-b_{\dot{\phi}}$, of order 15%, due to slotted walls, was considerably greater than with the previous models, and the effect on $-b_{\phi}$ corresponded to an upward displacement of the curve, instead of a downward displacement as for the other models.

Much larger values of $-b_{\phi}$ were obtained with the $A = 2$ rectangular wing than with the other models, all of which had larger aspect ratios and physically smaller sections. This suggested that the flow and hence the geometry at the tip might be important. To investigate this the effect of fairing the tip of the model was tried, a light wooden fairing being glued to the profile of the model at the tip. This had negligible effect on the frequency of oscillation but increased the aspect ratio and model area a small amount.

The result was to reduce the peak value of $-b_{\dot{\phi}}$ at $M = 0{\cdot}9$ by approximately 50% and introduce a region of negative damping between $M = 0{\cdot}9$ and $M = 1{\cdot}0$, where single-degree-of-freedom flutter was obtained (Fig. 14b). There was also a change in sign in the stiffness in this region, although this may have been present without the fairing, but the large dip at $M = 0{\cdot}9$ previously observed

without the fairing still remained. Measurements were made at the extremes of the flutter region where a steady amplitude of approximately 2 degrees was achieved, and values of the damping calculated by putting $x = 0$ in equation (5) (Section 3.2).

4.5. *Phase Angles* (36 *in.* × 14 *in. Tunnel Tests*).

The phase angle, ϵ, between the aerodynamic moment and the displacement is shown in Fig. 15 for each model, for a range of Mach numbers from 0·6 to 0·85 and for the slotted and closed conditions. In calculating the phase angles for the closed condition, values of b_ϕ uncorrected for tunnel interference have been used.

Below $M = 0{\cdot}8$, the change in phase angle between closed and slotted-tunnel conditions was not greatly influenced by Mach number and was approximately the same for the M-wing and tapered double wedge, whilst for the rectangular wings it was a little more than twice this value. The rectangular $A = 2$ wing behaved anomalously in that the phase angle decreased numerically when the slots were closed, whereas the other three wings showed an increase.

When the phase angle was close to 90 degrees the effect of sealing the slots was to produce a very much larger percentage change in the stiffness derivative than in the damping derivative. This suggested that the main interference effect was to produce a rotation of the aerodynamic moment vector by the amount shown in Fig. 15, rather than a change in the magnitude of the vector.

5. *Conclusions.*

(1) The derivatives varied smoothly with Mach number for the M-wing, but in the case of the tapered double wedge a numerical peak occurred in the region $0{\cdot}9 < M < 1$. The rectangular wings showed similar peaks together with large fluctuations in the transonic range.

(2) At the lower Mach numbers the results with slotted walls (36 in. × 14 in. Tunnel), compared with corrected results for the closed tunnel, showed increases in $-b_\phi$ by amounts varying up to 19% and, except with the M-wing, produced very large changes in $-b_\phi$.

The effect on $-b_\phi$ may be interpreted in general as resulting from a rotation of the aerodynamic moment vector, but in the case of the rectangular wing, $A = 2$, the rotation is in the opposite direction from that obtained with the other three wings.

(3) Theoretical values of $-b_\phi$ are in very good agreement with the M-wing measurements, but are in general low compared with results obtained for the remaining wings. Agreement is closest with measurements made under closed-tunnel conditions.

6. *Acknowledgement.*

The authors wish to record the helpful suggestions and assistance given by Mr. J. B. Bratt.

LIST OF SYMBOLS

A	Aspect ratio
B	Aerodynamic moment on model $= B_\phi\phi + B_{\dot\phi}\dot\phi$
b_ϕ, $b_{\dot\phi}$	Non-dimensional values of derivatives {*see* equations (6) and (7)}
$\bar{c}$	Mean chord
f	Frequency of oscillation
I	Inertia
p	Angular frequency $= 2\pi f$
S	Model wing area
s	Model wing span
t	Time
T	Period of oscillation
V	Wind speed
x	Logarithmic decrement
ϵ	Phase-angle lead of force on displacement
κ	Apparatus damping
λ	Taper ratio = tip chord/root chord
μ	Damping factor $= -2fx$
$\bar{\nu}$	Frequency parameter $= \dfrac{2\pi f\bar{c}}{V}$
ρ	Air density
σ	Elastic stiffness
$\bar{\phi}$	Amplitude of oscillation
	Suffix 0 relates to still-air conditions

REFERENCES

No.	*Author(s)*	*Title, etc.*
1	W. E. A. Acum	The comparison of theory and experiment for oscillating wings. (Prepared for the A.G.A.R.D. Manual on Aeroelasticity.) A.R.C. C.P. 681. March, 1962.
2	J. B. Bratt	Wind-tunnel techniques for the measurement of oscillatory derivatives. A.R.C. R. & M. 3319. August, 1960.
3	H. C. Garner and W. E. A. Acum ..	Interference corrections for asymmetrically loaded wings in closed rectangular wind tunnels. A.R.C. R. & M. 2948. September, 1953.
4	H. C. Garner and W. E. A. Acum ..	Theoretical subsonic derivatives for an oscillating M-wing. A.R.C. R. & M. 3214. January, 1959.

TABLE 1

M-Wing, 25 *in.* × 20 *in. Tunnel*

Slotted Tunnel				Closed Tunnel			
M	ω	$-b_{\dot{\phi}}$	$-b_{\phi}$	ω	$-b_{\dot{\phi}}$ (Uncorrected)	$-b_{\dot{\phi}}$	$-b_{\phi}$
0·6	0·0747	0·326	0·0259	0·0740	0·340	0·329	0·0272
0·7	0·0650	0·337	0·0230	0·0644	0·357	0·344	0·0233
0·8	0·0576	0·344	0·0214	0·0573	0·353	0·340	0·0235
0·85	0·0548	0·350	0·0263	0·0543	0·373	0·359	0·0213
0·9	0·0521	0·352	0·0163				
1·0	0·0477	0·368	0·0237				
1·1	0·0440	0·374	0·0169				

TABLE 2

M-Wing, 36 *in.* × 14 *in. Tunnel*

Slotted Tunnel				Closed Tunnel			
M	ω	$-b_{\dot{\phi}}$	$-b_{\phi}$	ω	$-b_{\dot{\phi}}$ (Uncorrected)	$-b_{\dot{\phi}}$	$-b_{\phi}$
0·6	0·0736	0·340	0·0213	0·0736	0·351	0·331	0·0258
0·7	0·0639	0·350	0·0192	0·0640	0·356	0·335	0·0236
0·8	0·0568	0·371	0·0183	0·0569	0·369	0·346	0·0217
0·85	0·0538	0·365	0·0187	0·0539	0·380	0·355	0·0211
0·9	0·0513	0·375	0·0188				
1·0	0·0469	0·376	0·0165				
1·1	0·0435	0·390	0·0213				

TABLE 3

Symmetrical Tapered Wedge

Slotted Tunnel				Closed Tunnel			
M	ω	$-b_{\dot{\phi}}$	$-b_{\phi}$	ω	$-b_{\dot{\phi}}$ (Uncorrected)	$-b_{\dot{\phi}}$	$-b_{\phi}$
0·6	0·0825	0·502	−0·0046	0·0830	0·520	0·480	+0·0022
0·7	0·0716	0·554	−0·0069	0·0720	0·561	0·514	−0·0016
0·8	0·0634	0·600	−0·0125	0·0637	0·625	0·566	−0·0081
0·85	0·0599	0·638	−0·0189	0·0603	0·752	0·666	−0·0174
0·9	0·0568	0·716	−0·0344				
1·0	0·0523	0·589	−0·0075				
1·1	0·0486	0·563	−0·0009				

TABLE 4

Rectangular Wing, $A = 4$

Slotted Tunnel				Closed Tunnel $f = 23$ c/sec			
M	ω	$-b_{\dot{\phi}}$	$-b_{\phi}$	ω	$-b_{\dot{\phi}}$ (Uncorrected)	$-b_{\dot{\phi}}$	$-b_{\phi}$
0·6	0·0939	0·540	−0·0157	0·0935	0·555	0·498	−0·0004
0·7	0·0812	0·573	−0·0207	0·0810	0·605	0·537	−0·0110
0·8	0·0714	0·664	−0·0438	0·0706	0·731	0·630	−0·0630
0·85	—	⩾0·792	—	0·0683	0·233	0·221	−0·0051
0·9	0·0669	−0·021	+0·0582				
1·0	0·0597	+0·608	−0·0040				
1·1	0·0555	+0·570	+0·0035				

Closed Tunnel $f = 33$ c/sec

M	ω	$-b_{\dot{\phi}}$ (Uncorrected)	$-b_{\dot{\phi}}$	$-b_{\phi}$
0·6	0·1175	0·539	0·485	+0·0164
0·7	0·1018	0·602	0·533	+0·0019
0·8	0·0888	0·741	0·625	−0·0651
0·85	0·0849	0·396	0·358	−0·0339

TABLE 5

Rectangular Wing, $A = 2$

Slotted Tunnel				Closed Tunnel			
M	ω	$-b_{\dot{\phi}}$	$-b_{\phi}$	ω	$-b_{\dot{\phi}}$ (Uncorrected)	$-b_{\dot{\phi}}$	$-b_{\phi}$
0·6	0·1211	0·422	−0·0065	0·1210	0·392	0·355	−0·0140
0·7	0·1049	0·451	−0·0121	0·1048	0·416	0·373	−0·0217
0·8	0·0926	0·500	−0·0283	0·0925	0·476	0·418	−0·0388
0·85	0·0874	0·521	−0·0504	0·0866	0·618	0·520	−0·0898
0·9	0·0814	0·753	−0·1176				
1·0	0·0772	0·198	+0·0012				
1·1	0·0707	0·485	−0·0260				

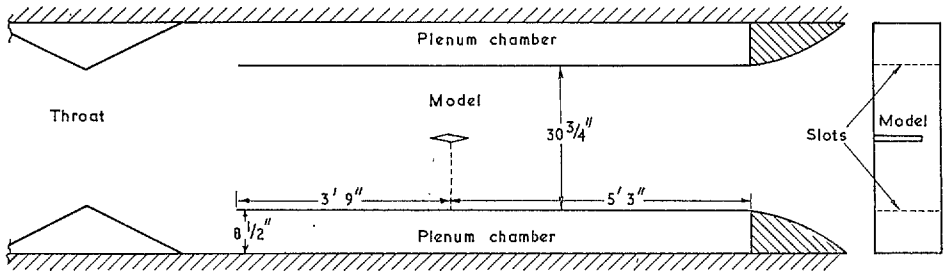

FIG. 1. 36 in. × 14 in. High Speed Tunnel.

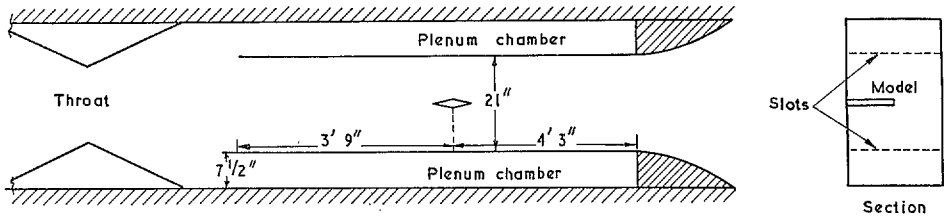

FIG. 2. 25 in. × 20 in. High Speed Tunnel.

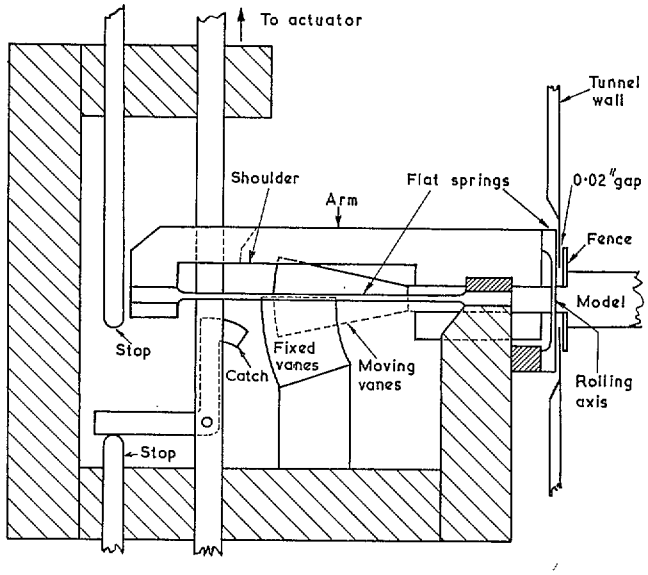

FIG. 3. Diagram of oscillation mechanism.

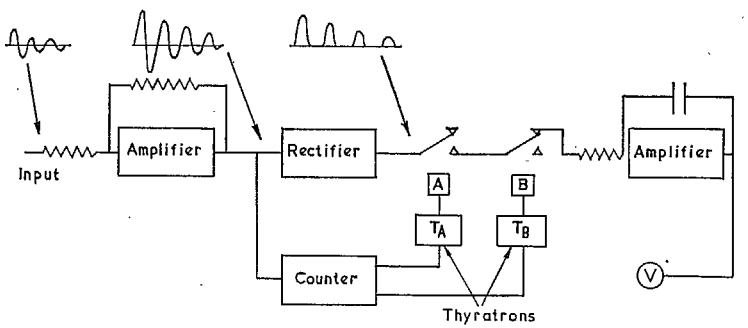

FIG. 4. Diagram of analyser.

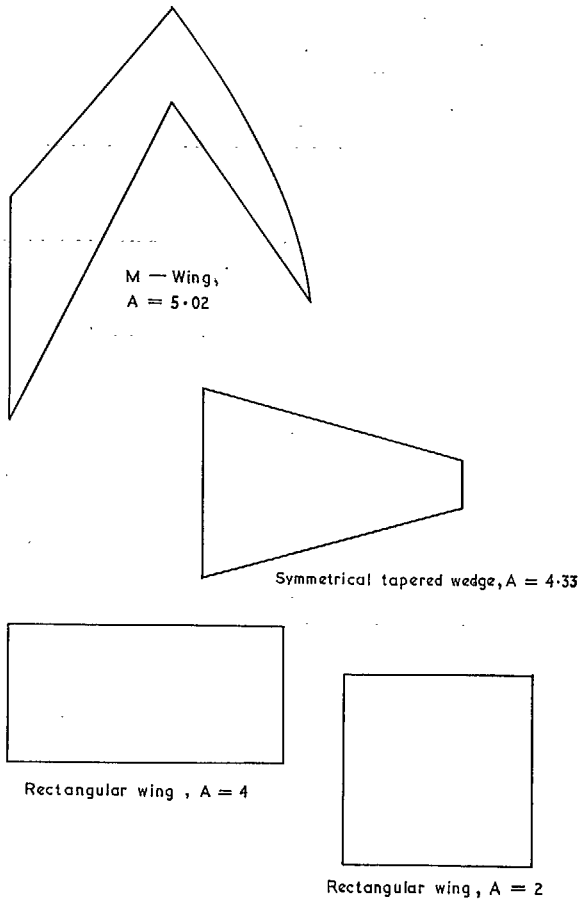

FIG. 5. Planforms of the models.

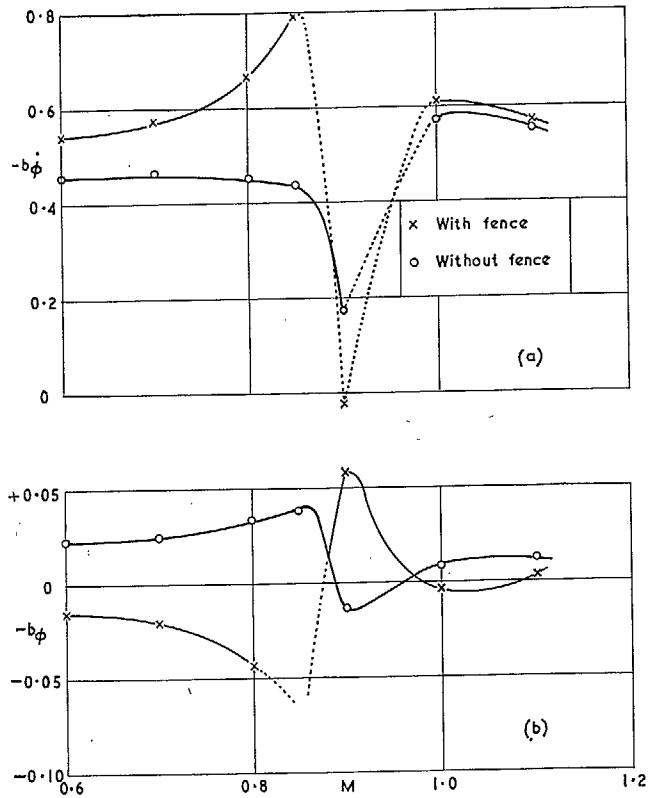

FIG. 6. Variation of $-b_{\phi}$ and $-b_{\dot{\phi}}$ with Mach number. Rectangular wing, A = 4.

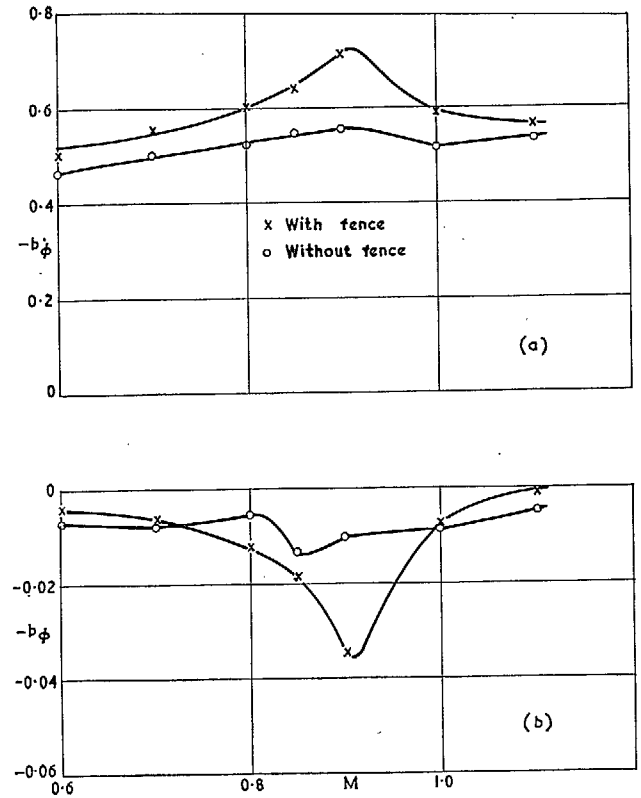

FIG. 7. Variation of $-b_{\phi}$ and $-b_{\dot{\phi}}$ with Mach number. Tapered double wedge.

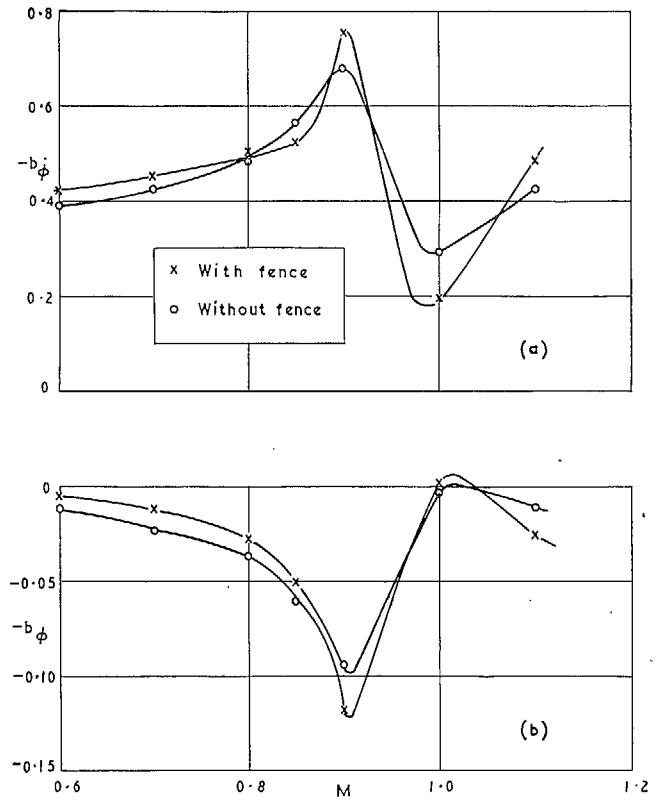

FIG. 8. Variation of $-b_\phi$ and $-b_{\dot\phi}$ with Mach number. Rectangular wing, $A = 2$.

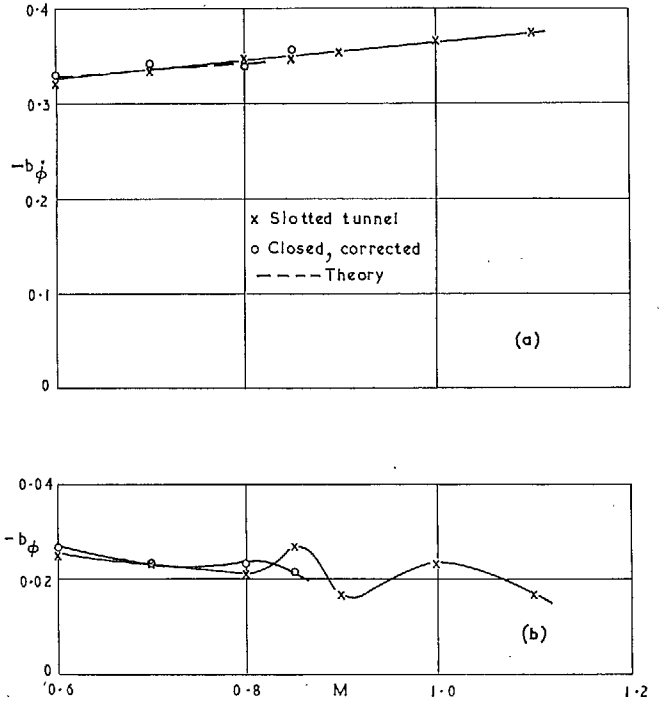

FIG. 9. Variation of $-b_\phi$ and $-b_{\dot\phi}$ with Mach number. M-wing, 25 in. × 20 in. Tunnel.

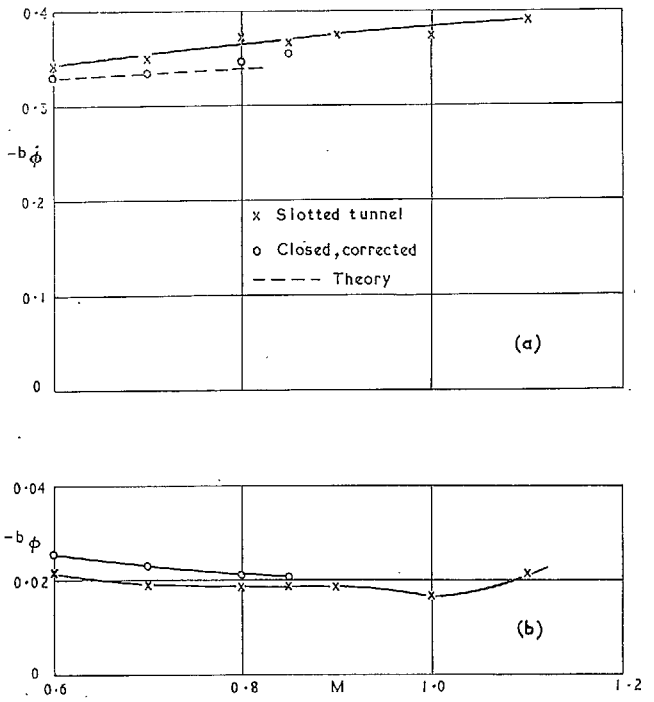

FIG. 10. Variation of $-b_\phi$ and $-b_{\dot{\phi}}$ with Mach number. M-wing, 36 in. × 14 in. Tunnel.

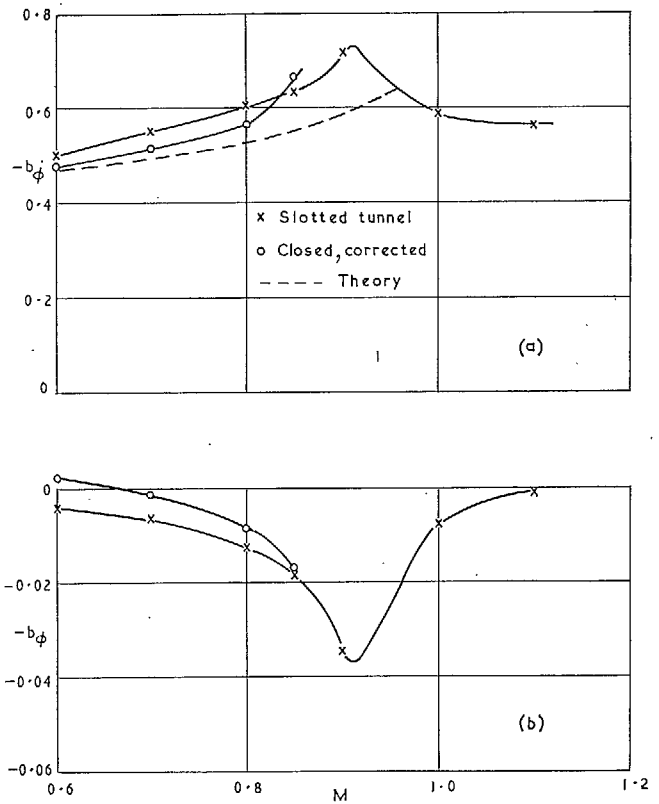

FIG. 11. Variation of $-b_\phi$ and $-b_{\dot{\phi}}$ with Mach number. Tapered double wedge.

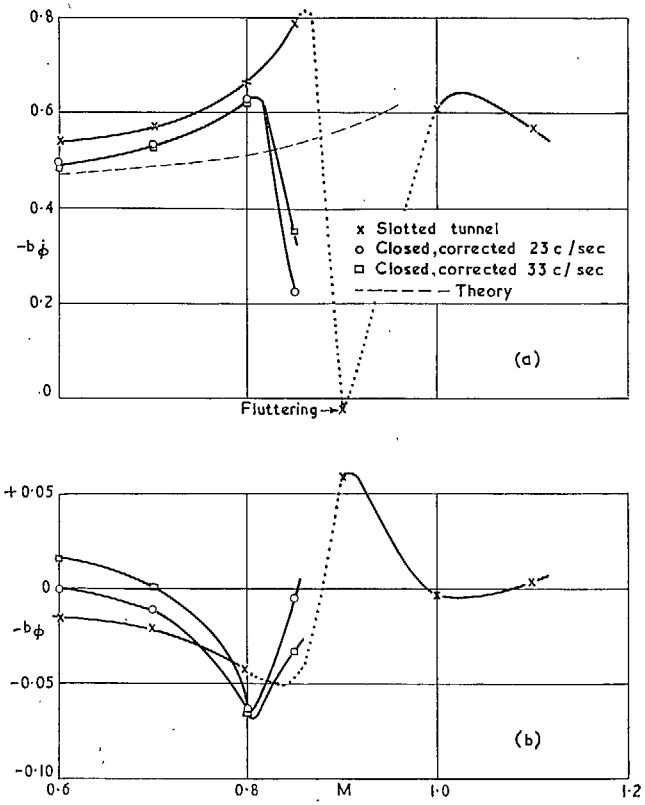

FIG. 12. Variation of $-b_\phi$ and $-b_{\dot{\phi}}$ with Mach number. Rectangular wing, $A = 4$.

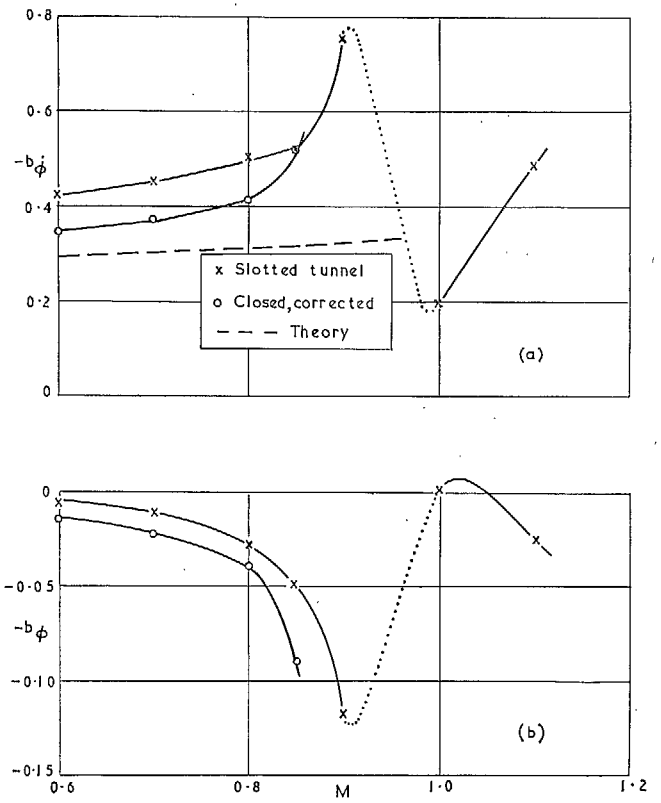

FIG. 13. Variation of $-b_\phi$ and $-b_{\dot{\phi}}$ with Mach number. Rectangular wing, $A = 2$.

(90062) Wt. 66/2301 K.5 9/64 Hw.

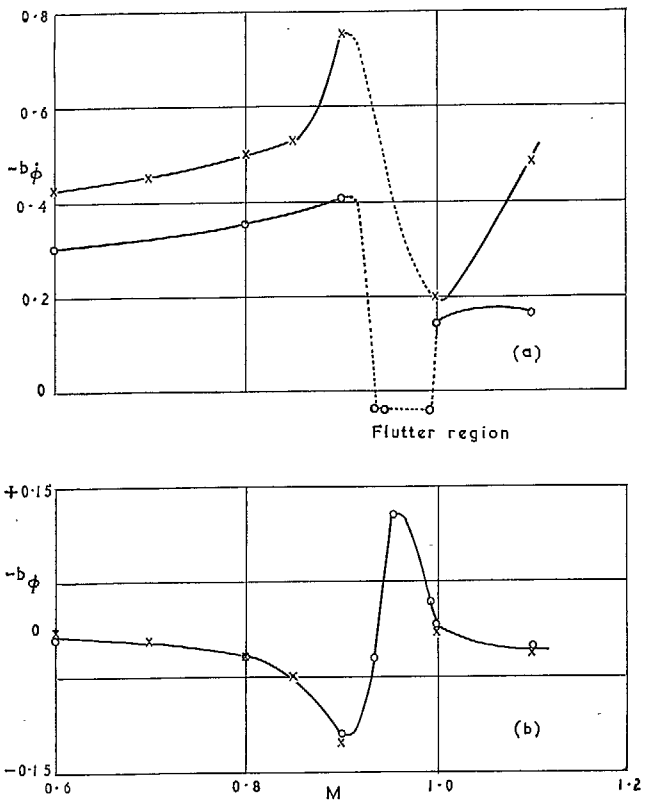

FIG. 14. Variation of $-b_{\phi}$ and $-b_{\dot{\phi}}$ with Mach number. Rectangular wing, $A = 2$, o normal, × with fairing.

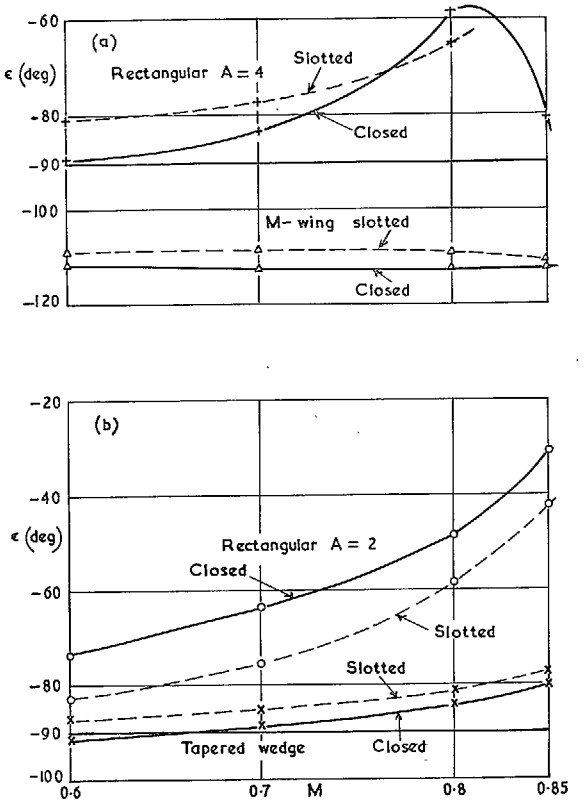

FIG. 15. Variation of phase angle with Mach number.

Publications of the Aeronautical Research Council

ANNUAL TECHNICAL REPORTS OF THE AERONAUTICAL RESEARCH COUNCIL (BOUND VOLUMES)

1942 Vol. I. Aero and Hydrodynamics, Aerofoils, Airscrews, Engines. 75*s.* (post 2*s.* 9*d.*)
Vol. II. Noise, Parachutes, Stability and Control, Structures, Vibration, Wind Tunnels. 47*s.* 6*d.* (post 2*s.* 3*d.*)

1943 Vol. I. Aerodynamics, Aerofoils, Airscrews. 80*s.* (post 2*s.* 6*d.*)
Vol. II. Engines, Flutter, Materials, Parachutes, Performance, Stability and Control, Structures. 90*s.* (post 2*s.* 9*d.*)

1944 Vol. I. Aero and Hydrodynamics, Aerofoils, Aircraft, Airscrews, Controls. 84*s.* (post 3*s.*)
Vol. II. Flutter and Vibration, Materials, Miscellaneous, Navigation, Parachutes, Performance, Plates and Panels, Stability, Structures, Test Equipment, Wind Tunnels. 84*s.* (post 3*s.*)

1945 Vol. I. Aero and Hydrodynamics, Aerofoils. 130*s.* (post 3*s.* 6*d.*)
Vol. II. Aircraft, Airscrews, Controls. 130*s.* (post 3*s.* 6*d.*)
Vol. III. Flutter and Vibration, Instruments, Miscellaneous, Parachutes, Plates and Panels, Propulsion. 130*s.* (post 3*s.* 3*d.*)
Vol. IV. Stability, Structures, Wind Tunnels, Wind Tunnel Technique. 130*s.* (post 3*s.* 3*d.*)

1946 Vol. I. Accidents, Aerodynamics, Aerofoils and Hydrofoils. 168*s.* (post 3*s.* 9*d.*)
Vol. II. Airscrews, Cabin Cooling, Chemical Hazards, Controls, Flames, Flutter, Helicopters, Instruments and Instrumentation, Interference, Jets, Miscellaneous, Parachutes. 168*s.* (post 3*s.* 3*d.*)
Vol. III. Performance, Propulsion, Seaplanes, Stability, Structures, Wind Tunnels. 168*s.* (post 3*s.* 6*d.*)

1947 Vol. I. Aerodynamics, Aerofoils, Aircraft. 168*s.* (post 3*s.* 9*d.*)
Vol. II. Airscrews and Rotors, Controls, Flutter, Materials, Miscellaneous, Parachutes, Propulsion, Seaplanes, Stability, Structures, Take-off and Landing. 168*s.* (post 3*s.* 9*d.*)

1948 Vol. I. Aerodynamics, Aerofoils, Aircraft, Airscrews, Controls, Flutter and Vibration, Helicopters, Instruments, Propulsion, Seaplane, Stability, Structures, Wind Tunnels. 130*s.* (post 3*s.* 3*d.*)
Vol. II. Aerodynamics, Aerofoils, Aircraft, Airscrews, Controls, Flutter and Vibration, Helicopters, Instruments, Propulsion, Seaplane, Stability, Structures, Wind Tunnels. 110*s.* (post 3*s.* 3*d.*)

Special Volumes

Vol. I. Aero and Hydrodynamics, Aerofoils, Controls, Flutter, Kites, Parachutes, Performance, Propulsion, Stability. 126*s.* (post 3*s.*)
Vol. II. Aero and Hydrodynamics, Aerofoils, Airscrews, Controls, Flutter, Materials, Miscellaneous, Parachutes, Propulsion, Stability, Structures. 147*s.* (post 3*s.*)
Vol. III. Aero and Hydrodynamics, Aerofoils, Airscrews, Controls, Flutter, Kites, Miscellaneous, Parachutes, Propulsion, Seaplanes, Stability, Structures, Test Equipment. 189*s.* (post 3*s.* 9*d.*)

Reviews of the Aeronautical Research Council

1939–48 3*s.* (post 6*d.*) 1949–54 5*s.* (post 5*d.*)

Index to all Reports and Memoranda published in the Annual Technical Reports

1909–1947 R. & M. 2600 (out of print)

Indexes to the Reports and Memoranda of the Aeronautical Research Council

Between Nos. 2351–2449	R. & M. No. 2450 2*s.* (post 3*d.*)
Between Nos. 2451–2549	R. & M. No. 2550 2*s.* 6*d.* (post 3*d.*)
Between Nos. 2551–2649	R. & M. No. 2650 2*s.* 6*d.* (post 3*d.*)
Between Nos. 2651–2749	R. & M. No. 2750 2*s.* 6*d.* (post 3*d.*)
Between Nos. 2751–2849	R. & M. No. 2850 2*s.* 6*d.* (post 3*d.*)
Between Nos. 2851–2949	R. & M. No. 2950 3*s.* (post 3*d.*)
Between Nos. 2951–3049	R. & M. No. 3050 3*s.* 6*d.* (post 3*d.*)
Between Nos. 3051–3149	R. & M. No. 3150 3*s.* 6*d.* (post 3*d.*)

HER MAJESTY'S STATIONERY OFFICE

from the addresses overleaf

© *Crown copyright* 1964

Printed and published by
HER MAJESTY'S STATIONERY OFFICE

To be purchased from
York House, Kingsway, London W.C.2
423 Oxford Street, London W.1
13A Castle Street, Edinburgh 2
109 St. Mary Street, Cardiff
39 King Street, Manchester 2
50 Fairfax Street, Bristol 1
35 Smallbrook, Ringway, Birmingham 5
80 Chichester Street, Belfast 1
or through any bookseller

Printed in England

S.O. Code No. 23-3376